Title

Multivariate social strategies buffer the fitness consequences of phenotype–environment mismatches

Authors:

Corné de Groot[1*†], Rori E. Wijnhorst[1†], Yimen G. Araya-Ajoy[2,3], Alastair J. Wilson[4], Henrik Jensen[2,3], Jonathan Wright[2], Niels J. Dingemanse[1]

Affiliations:

[1] Behavioural Ecology, Faculty of Biology, LMU Munich, 82152 Planegg-Martinsried, Germany

[2] Department of Biology, Norwegian University of Science and Technology (NTNU), N-7491 Trondheim, Norway

[3] Gjærevoll Centre, Norwegian University of Science and Technology (NTNU), N-7491 Trondheim, Norway

[4] Centre for Ecology and Conservation, College of Life and Environmental Sciences, University of Exeter, Penryn, UK

*Corresponding author contact information: c.degroot@bio.lmu.de

† These authors contributed equally to this work.

Author Contributions:

Designed research: N.J.D., J.W., Y.G.A., R.E.W, C.dG

Collected data: C.dG, R.E.W.

Performed research: C.dG, R.E.W., N.J.D.

Contributed analytic tools: Y.G.A., A.J.W.

Analyzed data: C.dG

Wrote the paper: C.dG, R.E.W., N.J.D.

Reviewed and commented on manuscript: A.J.W., H.J., Y.G.A., J.W.

Competing Interest Statement: the authors declare no competing interests.

Classification: Biological sciences, Evolution

Key words:

- Phenotypic integration
- Selection
- Phenotypic plasticity
- Social evolution
- Foraging

Abstract

How organisms adapt to environmental change is a fundamental question in biology. Environmental shifts frequently induce mismatches between an organism's phenotype and its surroundings, including the social environments created by interacting individuals. Such mismatches can be mitigated by modifying one's own phenotype through plasticity, adjusting the environment, or selecting environments matching intrinsic phenotypes. Using a wild passerine bird model, we investigated social foraging under negative frequency-dependent selection, where fitness is determined by the proportion of individuals searching for food ("producing") versus exploiting others ("scrounging"). Because individuals possess distinct and repeatable behavioral types, they experience unique phenotype–environment mismatches relative to this landscape. By experimentally manipulating group compositions, we estimated how house sparrows integrate plasticity and environmental modification to mitigate these mismatches. We show that individuals adjusted their own foraging tactics while simultaneously eliciting behavioral changes in partners. These responses varied among individuals and are integrated with behavioral types, but their combined effect on phenotypic expression did not shift the population toward the fitness peak, which was already closely approximated by the population mean. Instead, this multivariate strategy attenuated the fitness consequences of phenotype–environment mismatches by redistributing fitness among individuals: those furthest from the peak gain fitness, whereas those closest to it lose fitness. Consequently, social responsiveness and social impact reduced among-individual variation in fitness by 47%, weakening the selective differences that would otherwise drive evolutionary change. Broadly, our findings reveal how coordinated responses to social environments can stabilize individual fitness outcomes while constraining the evolutionary consequences of behavioral variation.

Significance statement

Predicting how life adapts to environmental change is a cornerstone of biology. Individuals can respond to phenotype–environment mismatches by altering their phenotype, modifying their environments, or selecting appropriate environments. Because individuals possess distinct behavioral types, they experience unique mismatches with their (social) environments. Using the social foraging producer-scrounger paradigm, we show that house sparrows deploy individual-specific multivariate strategies that combine social responsiveness (adjusting their own behavior) with social impact (eliciting behavioral changes in partners). This coordinated strategy equalizes foraging success among individuals and flattens the selective landscape, eliminating the selection pressure that would otherwise drive evolutionary change toward the fitness peak. Integrated behavioral strategies may therefore offer a general explanation for evolutionary stasis and the maintenance of phenotypic variation.

Introduction

Predicting how organisms reach adaptive peaks on complex fitness landscapes is a central challenge in biology (1–3). Classically, evolutionary adaptation is viewed as the result of natural selection acting on heritable traits across generations (4–6). However, organisms also possess other pathways to respond to phenotype–environment mismatches (1). Individuals can respond by adjusting their own phenotypes through plasticity (7, 8), actively modifying their environments to better match their phenotypes (9, 10), or selecting environments that suit their existing traits (3, 11). While these pathways are often studied in isolation, they serve a common adaptive function: reducing the costs of being mismatched with the environment. Because these mechanisms operate on the same fitness landscape, they should be considered as potentially integrated components of individual strategies rather than independent modules (1, 3, 12).

Social interactions provide an ideal model to test this integration because they create environments that are themselves shaped by the phenotypes of interacting individuals. In social contexts, an individual's environment consists largely of the phenotypes expressed by others (13, 14). Under negative frequency-dependent selection, fitness is interactively shaped by an individual's own phenotype and the social environment it experiences. A classic paradigm for such social dynamics is the producer–scrounger game, where individuals balance searching for food independently ("producing") with exploiting discoveries made by others ("scrounging") (15, 16). Because the optimal strategy depends on the behavior of social partners, individuals with different behavioral types will experience different phenotype–environment mismatches. Such mismatches will thus generate fitness differences among behavioral types, which over evolutionary time will deplete variation in behavioral types unless other mechanisms mitigate these fitness differences. Navigating these social fitness landscapes therefore requires individuals to both alter their own phenotype in response to their social environment ("social responsiveness") and influence the phenotypes expressed by their partners ("social impact") (12, 17–21). Social responsiveness represents a form of phenotypic plasticity (12, 14, 17), whereas social impact represents a form of environmental modification through indirect effects on interacting individuals (12, 21, 22).

Despite being plastic, behaviors are often also repeatable where individuals consistently differ from one another in their average behavioral phenotypes across repeated observations (23). Such behavioral types also occur in social foraging contexts, where producing and scrounging tactics can exhibit stable individual differences (24, 25). Consequently, individuals differ not only in their baseline behavioral types, but potentially also in how they respond to, and influence, their social environments (12, 18). These components may therefore form integrated, individual-specific strategies where behavioral types determine the initial phenotype-environment mismatch experienced by individuals, while responsiveness and impact determine how individuals alter the phenotype–environment combinations they experience.

Identifying how individuals navigate fitness landscapes requires the decomposition of variation in social foraging phenotypes into these constituent components (Fig. 1A-B). Because an individual's expressed phenotype emerges from the combination of its behavioral type, social responsiveness and social impact, selection acting on observed behaviors may indirectly shape these underlying components (1, 26). We therefore expect that these components are functionally integrated (12, 18), generating coordinated multivariate strategies that allow individuals to respond to phenotype–environment mismatches (1). By experimentally manipulating group compositions (Fig. 1C), we broke naturally occurring associations that

likely exist among individuals of certain types. This allowed us to isolate individual-specific behavioral components while controlling the social environments individuals encountered (19, 27).

Here, we quantify the fitness landscape of social foraging to test how behavioral types and individual-specific responses shape adaptation in a competitive social environment. We first characterize the relationship between individual and partner phenotypes generating the fitness landscape. We then test whether behavioral type, social responsiveness, and social impact are integrated into multivariate strategies. Finally, we determine how these strategies alter individual fitness outcomes. We show that individuals use coordinated behavioral responses to phenotype–environment mismatches. These responses reduce fitness differences among individuals, thereby weakening the selection that would otherwise drive evolutionary change.

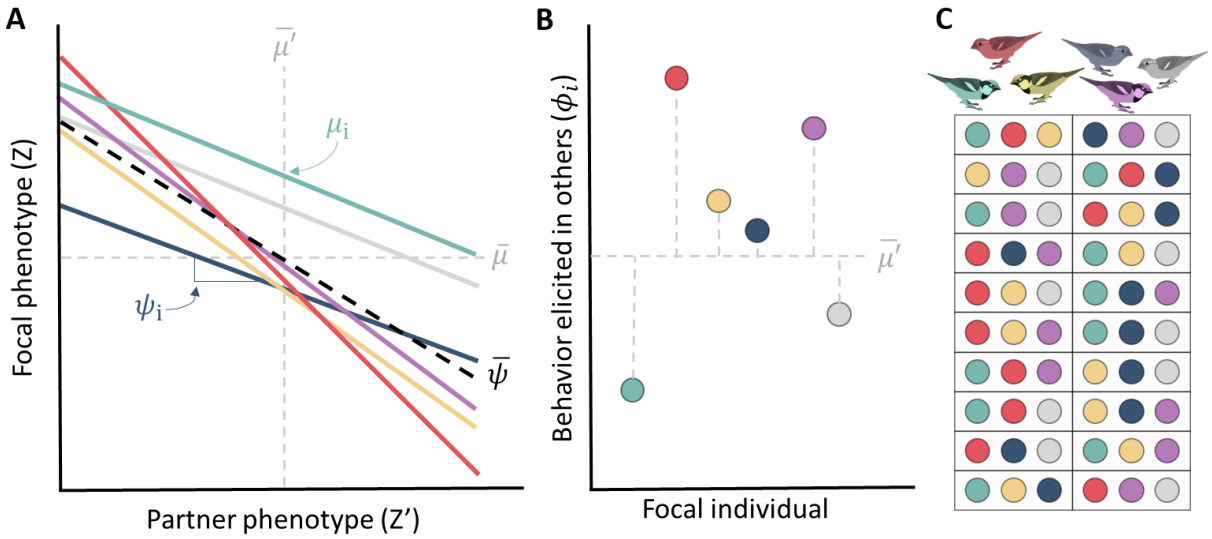

Fig. 1. Phenotypic decomposition of social behaviors and experimental design. A) *Social reaction norms describing how focal behavior (Z) changes as a function of partner behavior (Z'). The horizontal dashed grey line ($\bar{\mu}$) represents the population mean behavioral type, the vertical dashed grey line ($\bar{\mu}'$) the average social environment, and the dashed black line ($\bar{\psi}$) the population mean social responsiveness (the slope of the population-mean reaction norm). Individual social reaction norms (colored lines) decompose expressed behavioral phenotypes into behavioral type (μ_i; the intercept at the average social environment) and individual differences in social responsiveness (ψ_i; variation in reaction norm slopes).* ***B)*** *Social impact (ϕ), representing the degree to which an individual (i) on average elicits changes in partner behavior relative to the population mean ($\bar{\mu}'$).* ***C)*** *Experimental manipulation of social environments used to estimate individual-specific reaction norms and social impacts. Triads of wild house sparrows played social foraging games for 15 minutes using a 36-well checkerboard feeder – see Methods. Individuals were exposed to diverse social environments by playing each of 20 unique combinations of triads within a group of six individuals twice over two days.*

Results

Fitness Landscapes for Social Foraging

To characterize the fitness landscape of social foraging, we analyzed foraging success as the fitness currency of the producer–scrounger game (15, 16). Our results revealed a positive directional component

of natural selection ($\beta_1 > 0$) towards increased scrounging, combined with negative quadratic selection ($\gamma_{11} < 0$), resulting in a stabilizing fitness surface around an optimum (Fig. 2A). Similarly, social selection induced by partner behavior showed a positive directional component ($\beta_2 > 0$) and negative quadratic component ($\gamma_{22} < 0$), indicating stabilizing selection for an optimal social environment (Fig. 2A). Individuals achieved peak foraging success at a scrounging proportion of 0.347 (95% CI: 0.324–0.366) within social environments where partners expressed an average proportion of 0.377 (95% CI: 0.358–0.402). A negative interaction between natural and social selection gradients ($\gamma_{12} < 0$; Fig. 2A) provided evidence for negative frequency-dependent selection (15, 16). Because the ratio $(\gamma_{11}\gamma_{22})/{\gamma_{12}}^2$ exceeded one (4.08, 95% CI: 2.654–6.941), stabilizing curvature along the phenotype and social-environment axes outweighed the negative interaction, resulting in a distinct topological fitness peak rather than a saddle (28). This establishes a frequency-dependent landscape where optimal strategies depend on the social environment, creating selection for individuals to respond to phenotype–environment mismatches.

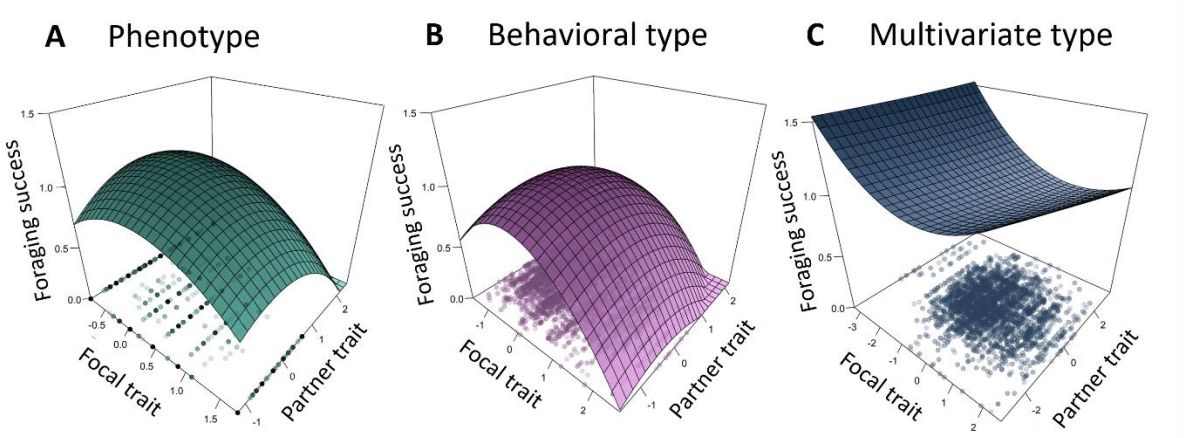

	Selection gradient (95% CI)	Selection gradient (95% CI)	Selection gradient (95% CI)
β_1	0.035 (0.014 ; 0.056)	-0.012 (-0.051 ; 0.028)	-0.032 (-0.062 ; -0.001)
β_2	0.049 (0.033 ; 0.066)	-0.028 (-0.050 ; -0.005)	-0.034 (-0.051 ; -0.017)
γ_{11}	-0.177 (-0.214 ; -0.138)	-0.133 (-0.291 ; 0.030)	0.039 (-0.004 ; 0.081)
γ_{22}	-0.115 (-0.142 ; -0.087)	-0.082 (-0.186 ; 0.022)	0.001 (-0.021 ; 0.023)
γ_{12}	-0.070 (-0.090 ; -0.051)	-0.012 (-0.034 ; 0.010)	-0.010 (-0.026 ; 0.007)

Figure 2. Fitness landscapes for producer–scrounger phenotypes. *Fitness surfaces based on z-standardised posterior median selection gradient parameters for:* ***A)*** *observed proportion of scrounging events;* ***B)*** *behavioral type (individual mean proportion of scrounging events); and* ***C)*** *multivariate type, represented by latent variable factor scores describing an integrated producer–scrounger strategy. Latent variable scores are inverted so that higher values indicate more scrounger-oriented strategies relative to Figure 3. Foraging success is relativized by dividing by the arithmetic mean. Fitness surfaces are truncated at zero, with predicted phenotypes of focal individuals and social partners projected onto the floor within the observed parameter space. Posterior median selection gradient estimates with 95% credible intervals are shown below each panel, where β represents linear and γ nonlinear selection parameters. Subscript "1" denotes selection on focal phenotypes and subscript "2" denotes social selection imposed by partner phenotypes. Quadratic selection gradients are doubled following standard practice* (29)*. See SI Appendix Table S1 for all model estimates. Analyses based on 5002 observations of 245 individuals.*

Individual Responses to Social Mismatches

Decomposing phenotypic variation revealed that sparrows responded to phenotype–environment mismatches by simultaneously altering their own behavior and influencing their social environment. First, repeatable individual differences in average producing and scrounging across trials confirmed distinct behavioral types (Fig. 3A). Second, birds adjusted their scrounging through negative frequency-dependent social responsiveness, increasing producing ($\bar{\psi}$ = 2.564, 95% CI: 2.356–2.769) and decreasing scrounging ($\bar{\psi}$ = −2.034, 95% CI: −2.138 to −1.925) when group members scrounged more (SI Appendix, Table S2). Social responsiveness differed among individuals for producing, but not scrounging behavior (Fig. 3A). Third, focal identity significantly affected partner behavior (Fig. 3A), demonstrating stable differences in social impact, whereby some individuals consistently elicited higher producing or scrounging from their partners than others (19, 22). Together, variation in behavioral type, social responsiveness, and social impact indicate that individuals differ not only in their baseline phenotypes, but also in how they respond to and shape their social environments.

Multivariate Integration of Behavioral Type, Social Responsiveness, and Social Impact

We used structural equation modeling (SEM) to evaluate whether behavioral type, social responsiveness, and social impact represent independent components or an integrated strategy (30). This approach evaluated five alternative multivariate structures (SI Appendix, Figure S2) describing the dataset characterized by 15 pairwise correlations among six behavioral components (Fig. 3A; SI Appendix, Figure S1). The best-supported model described behavioral type, social responsiveness, and social impact for both foraging tactics as expressions of a single latent axis of among-individual variation (Fig. 3B). Individuals scoring high on this latent variable possessed a behavioral type inclined towards producing, but also exhibited stronger social responsiveness by increasing their producing behavior more when partners had higher scrounging rates. Critically, these same individuals also exerted a distinct social impact, eliciting higher scrounging from partners. This coordinated pattern demonstrates that behavioral type, social responsiveness, and social impact are not independent components, but instead form integrated multivariate individual social strategies.

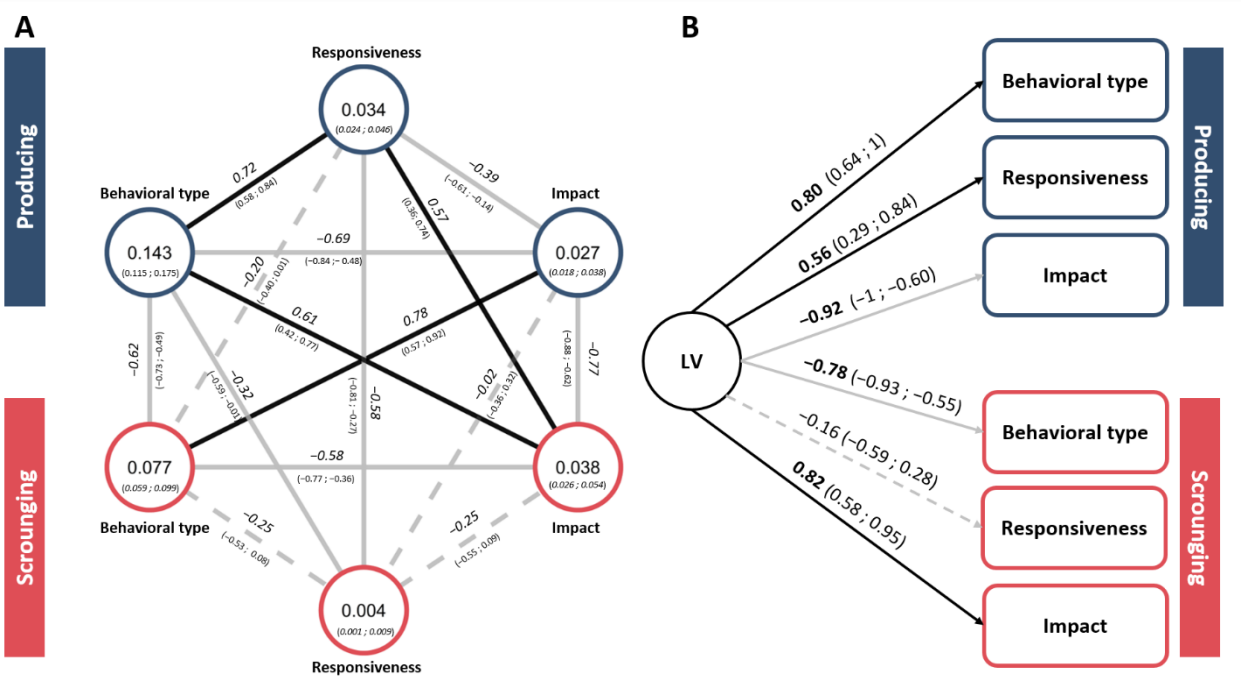

Figure 3. Integration of producer–scrounger phenotypic components. *Individual variation was decomposed into six components: behavioral type, social responsiveness, and social impact; each for producing and scrounging behavior (blue and red, respectively). Black and grey arrows indicate positive and negative correlations, respectively. Solid and dashed lines indicate whether correlations have 95% credible intervals excluding or overlapping zero. Estimates are posterior medians with 95% credible intervals. Analyses based on 5002 observations of 245 individuals.* ***A)*** *Correlation network showing relationships among components. Nodes show among-individual repeatability estimates, and edges correlations (95% credible intervals).* ***B)*** *Structural equation model (SEM) that was best-supported (see SI Appendix Figure S1), showing integration of components into a latent producer–scrounger strategy. Estimates represent standardized loadings onto latent variables (LV).*

Multivariate Types Redistribute Predicted Fitness

To quantify the adaptive consequences of multivariate types, we predicted each individual's phenotype and social environment under distinct scenarios (SI Appendix, Table S3): (i) assuming individuals expressed only their behavioral type; or (ii) their multivariate type, incorporating individual-specific behavioral type, social responsiveness and social impact. We then estimated predicted relative foraging success by projecting each phenotype–environment combination onto the fitness landscape (Fig. 2A).

These projected phenotype–environment combinations were close to the fitness peak under both scenarios (Fig. 4A), indicating that the average individual already occupied a near-optimal region of the fitness landscape. Nevertheless, predicted fitness changed markedly among individuals (Fig. 4B). Compared with just behavioral types, the average relative foraging success of multivariate types decreased by 2.15% (95% CI: 1.29–3.02%), while among-individual variance in predicted fitness decreased by 47.1% (95% CI: 19.9–64.6). Random regression analyses revealed that this reduction resulted from individuals with low predicted fitness in the behavioral type only scenario increasing their fitness in the multivariate type scenario, whereas those with high predicted fitness showed the opposite response

(intercept–slope correlation (*r*) = -0.64, 95% CI: -0.80 to -0.46). Thus, individual-specific social responsiveness and social impact redistributed predicted fitness among behavioral types while leaving the average phenotype–environment combination close to the fitness peak.

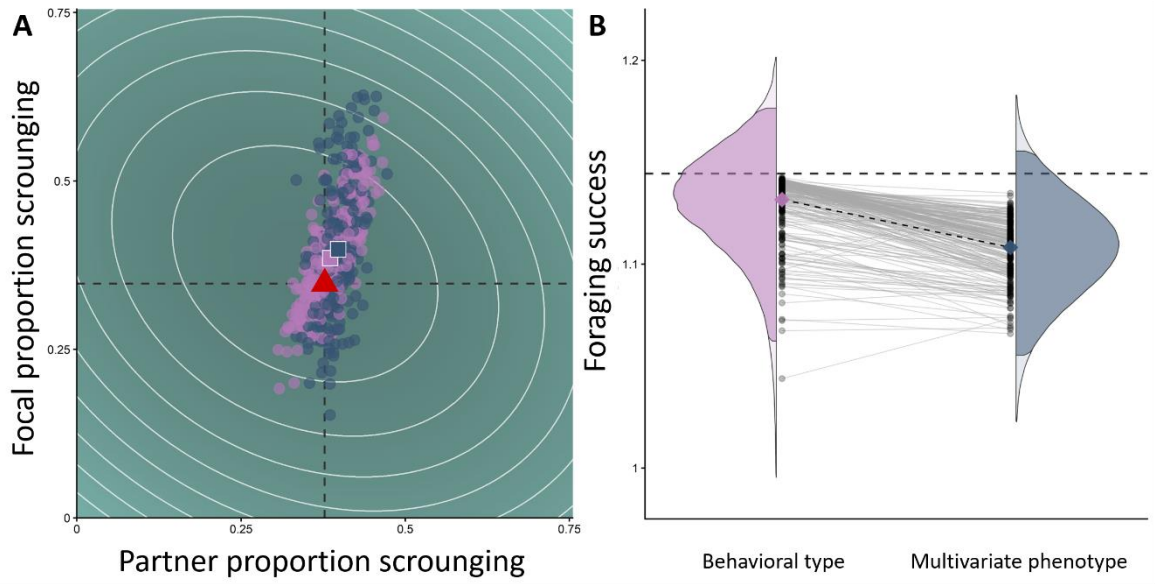

Figure 4. Predicted fitness consequences for behavioral types versus multivariate phenotypes. *Predicted phenotype–environment combinations and associated relative foraging success assuming individuals expressed only their behavioral types (purple) or their multivariate types (blue). Analyses based on 5002 observations of 245 individuals.* ***A)*** *Posterior median two-dimensional fitness landscape (as in Fig. 2A) with the fitness peak (red triangle), posterior median individual means (colored points), and posterior median population mean predicted phenotype–environment combinations (colored squares). Contours represent 5% intervals in relative foraging success (i.e. fitness).* ***B)*** *Predicted relative foraging success under both scenarios. Points show posterior median individual mean estimates connected by reaction norms (grey). Half violins represent the 95% (opaque) and 99% (transparent) posterior distributions of individual predicted means. The horizontal dashed line indicates predicted relative foraging success at the fitness peak.*

Behavioral Responses Flatten the Selection Landscape

The evolutionary consequence of this redistribution of predicted individual foraging successes (Fig.4B) was evident in the curvature of the fitness landscape. When characterized using phenotypes expressed during trials or estimated behavioral types, the surface exhibited high curvature (Frobenius norm = 0.233, 95% CI: 0.194–0.274, and 0.167, 95% CI: 0.044–0.317, respectively; Fig. 2A-B), reflecting substantial fitness penalties for phenotype–environment mismatches. However, characterizing the landscape using the individual multivariate strategy scores from the best-fitting SEM largely eliminated this curvature (norm = 0.044, 95% CI: 0.014–0.084; Fig. 2C). This flattening demonstrates that integrating behavioral type with social responsiveness and social impact allows divergent behavioral profiles to achieve similar foraging success. By reducing fitness differences among individuals, these integrated strategies weaken the strength of selection acting on behavioral variation, providing a mechanistic explanation for evolutionary stasis.

Discussion

Our study shows that social foragers mitigate phenotype–environment mismatches through integrated multivariate strategies that combine behavioral type, social responsiveness, and social impact. Evolutionary theory has long recognized that organisms can reduce phenotype–environment mismatches by modifying their own phenotype through plasticity, altering their environment, or selecting environments that better match their phenotypes (1–3). While these pathways are typically considered independently, our results demonstrate that, in a social context, at least two of them, plasticity and environmental modification, are tightly integrated with individual social behavior. Rather than simply moving individuals toward the fitness optimum, these coordinated responses redistributed fitness among individuals. That is, those individuals furthest from the optimum gained fitness, whereas those initially closest to the optimum lost fitness. Consequently, integrated social strategies reduced fitness differences among behavioral types, weakening the selection that would otherwise drive evolutionary change in these social traits.

Our findings extend classical producer–scrounger theory by revealing that individuals navigate frequency-dependent fitness landscapes through more than behavioral plasticity alone (13, 15, 16). Previous work has established that stable individual differences in producing and scrounging can persist under negative frequency-dependent selection, because the optimal tactic depends on the behavior of social partners (15, 16, 24, 25). Our results support this prediction by demonstrating a fitness landscape in which optimal foraging success depended jointly on an individual's own behavior and that of its social partners. However, individuals did not simply adjust their own behavior to changing social environments. They simultaneously altered the behavior expressed by social partners, thereby modifying the very environment to which they were responding. This combination of social responsiveness and social impact extends concepts of indirect effects in social evolution (12, 14, 17–20, 22) by showing that both components contribute to how individuals navigate fitness landscapes.

More broadly, our results suggest that behavioral type, plasticity, and environmental modification should not be viewed as independent properties of individuals, but as integrated components of adaptive strategies. Behavioral ecology has traditionally treated consistent individual behavioral differences and behavioral plasticity as complementary, but distinct sources of phenotypic variation (23, 31). Likewise, environmental modification has generally been studied separately through concepts such as niche construction, indirect social effects or extended phenotypes (9, 10, 12, 22). By contrast, our structural equation analyses revealed that these components covary along a single axis of among-individual variation. Individuals therefore differed not simply in their average foraging behavior, but in a coordinated suite of traits linking baseline behavioral type with predictable patterns of social responsiveness and social impact. These findings imply that understanding how behavioral variation evolves requires considering the integrated strategies through which individuals both respond to and modify their environments, rather than studying these processes in isolation (1).

Importantly, these integrated strategies did not substantially improve the population average mismatch with the fitness peak. The phenotype–environment combinations were already centered close to the optimum when individuals expressed only their behavioral types. Instead, social responsiveness and social impact reduced the fitness costs of individual phenotype–environment mismatches by redistributing fitness among individuals. This distinction has broader implications for how adaptive plasticity is viewed.

Plastic responses are often interpreted as mechanisms that allow populations to track environmental optima, thereby buffering populations until natural selection produces genetic adaptation (7, 8, 32, 33). Our results instead demonstrate that plasticity, when integrated with environmental modification, can primarily function to buffer the costs of mismatches. In this case, adaptation is not achieved by the whole population moving closer to the optimum, but by reducing the fitness penalties associated with occupying different positions on the fitness landscape (33, 34).

Why would individuals already close to the fitness optimum adopt a strategy leading to reductions in expected fitness? Although our experiment was not designed to distinguish among mechanisms, several non-exclusive adaptive explanations are plausible. Maintaining a strong competitive advantage may itself be costly on the long-term, if it requires escalating conflict or continually resisting the behavioral influence of competitors (35–37). Accepting a modest reduction in immediate foraging success may therefore maximize longer-term fitness, if the costs of maintaining dominance outweigh the additional benefits of fewer contests. Alternatively, reducing disparities in foraging success may contribute to the persistence or cohesion of social groups, yielding future benefits through continued access to information, repeated cooperative interactions or reduced conflict with familiar social partners (38, 39). While selection acts on lifetime reproductive success rather than short-term foraging returns, integrated behavioral strategies may contribute to long-term fitness across the diverse social environments encountered over an individual's lifetime (40, 41). Distinguishing among these possibilities represents an important direction for future work.

Integrated social strategies also altered the evolutionary properties of the fitness landscape. Although behavioral types alone generated pronounced variation in expected fitness, incorporating social responsiveness and social impact substantially reduced this variation and flattened the landscape experienced by multivariate strategies. The immediate consequence is that phenotype–environment mismatches were minimized, a key mechanism by which adaptive plasticity is predicted to increase both population viability and alter the course of adaptive evolution (33, 34). The longer-term consequence is that the selective differences driving evolutionary change are weakened. Our findings therefore illustrate how short-term plastic behavioral responses can reduce the strength of natural selection without altering the underlying frequency-dependent structure of the fitness landscape. Such buffering mechanisms may help explain why consistent behavioral variation often persists despite evidence that behavioral types influence fitness (42, 43).

Finally, our study provides a broader framework for understanding how multiple adaptive pathways interact. By experimentally manipulating social environments, we were able to isolate the contributions of plasticity and environmental modification while controlling for agency in choice of (social) environment, a third major pathway for reducing phenotype–environment mismatches (1–3). In social systems, selecting environment often takes the form of non-random assortment among social partners (27, 44), making its integration with behavioral type, social responsiveness, and social impact a natural direction for future research. More broadly, our results suggest that organisms may navigate complex fitness landscapes not through single adaptive mechanisms, but through integrated multivariate strategies that simultaneously modify themselves and the environments they experience. Together, these integrated social strategies can reduce the fitness consequences of phenotype–environment mismatches, weaken selection, and thereby promote the long-term coexistence of multiple behavioral types.

Methods

Study population

Data were collected during the winters of 2022 and 2023 from a house sparrow (*Passer domesticus*) meta-population in Åfjord, Trøndelag, Norway. We caught birds using mist nets at five dairy farms separated by an average of 4.2 ± 0.64 km and characterized by limited dispersal (45). Captured birds were housed in indoor aviaries (2 × 1.5 × 2 m) in an unused dairy farm, provided with *ad libitum* food and water. Aviaries were maintained at 10 ± 2°C under a 14:10 h light:dark cycle, matching winter conditions in local dairy farms (45). We housed birds in groups of six with approximately equal sex ratios based on capture order. Groups were habituated over three days, and trained to forage from a checkerboard feeder containing food mixed into sand-filled wells following de Groot et al. (46). Afterwards, birds were recaptured and transferred overnight to the experimental setup in groups of three with *ad libitum* food.

Experimental setup

Producer–scrounger trials were conducted using three 36-well checkerboard feeders (1 × 1.2 × 1 m) housed within visually isolated wire-mesh cages equipped with a perch and *ad libitum* water. Each well was fitted with four RFID antennae that recorded the presence of multiple PIT-tagged birds every 0.5 s. We manipulated social environments by systematically varying the composition of triads. All 20 possible triadic combinations within each group of six individuals were tested over one day (Fig. 1C), and repeated on the following day. Trials lasted 15 min and were conducted between 08:20 and 17:35, separated by 25-min rest intervals. Every second trial, one triad was not played to prevent satiation.

Before each trial, all 36 interchangeable wells were filled to approximately 85% capacity with fine sand, of which 14 contained a total of 12 g millet buried at a depth of 1 cm. Baited wells randomly followed one of twelve randomized spatial configurations. Following each trial, birds were recaptured individually using remotely operated nest boxes, identified using RFID scanners, and assigned to their next triad according to a randomized daily schedule. Feeders were cleaned between trials, and all remaining sand and seed were removed. After completion of the first day, birds remained overnight in the experimental cages with food provided *ad libitum* using 28 baited wells containing 40 g millet. Following the second day of trials, groups were transferred to a large holding aviary (10 × 5 × 2 m) for monitoring before being released at their capture sites within 14 days.

We derived behavioral measures from RFID recordings that were calibrated with video observations from 180 trials (46). We quantified producing (number of food patches first discovered by an individual; r = 0.67), scrounging (number of patches joined after discovery by another individual; r = 0.72), and foraging success (number of seeds consumed; r = 0.80).

Statistics

We conducted 2,120 producer–scrounger trials with 245 individuals, yielding 6,360 individual observations where each bird acted both as a focal individual and as a social partner (35). Analyses were restricted to trials where all three individuals were detected by the RFID system and the focal individual, together with at least one social partner, expressed non-zero producing or scrounging behavior, resulting in 5,002 observations. Unless otherwise stated, all analyses were performed using Bayesian mixed-effects models implemented in Stan (47), with standardized continuous data. We specified weakly informative

Gaussian priors (μ = 0, σ = 1) for fixed effects, half-exponential priors (λ = 3) for variance components, and LKJ priors (η = 1.5) for correlation matrices.

Social responsiveness and social impact models

We estimated individual differences in behavioral type, social responsiveness, and social impact using mixed-effects models following Wijnhorst et al. (19). Behavioral type was defined as an individual's expected producing or scrounging phenotype in the average social environment (31), whereas social responsiveness quantified how an individual's phenotype changed as a function of the average phenotype expressed by its social partners (Equation 1.1). Models therefore estimated both an individual-specific intercept (behavioral type) and an individual-specific reaction norm slope (social responsiveness).

$$z1_{it} = \mu + \mu_i + (\bar{\psi} + \psi_i) * \left(\frac{x'_{jt} + x'_{kt}}{m}\right) + \left(\varepsilon_j + \varepsilon_k\right) + e_{it} \qquad \textit{Equation 1.1}$$

$$x_{it} = \mu + x_i + e_{it}$$

$$\begin{pmatrix} \mu_i \\ \psi_i \\ \varepsilon_i \\ x_i \end{pmatrix} \sim MVN(0, \Omega)\ \Omega: \begin{pmatrix} \sigma^2\mu_i & \sigma\mu_i,\psi_i & \sigma\mu_i,\varepsilon_i & \sigma\mu_i,x_i \\ \sigma\psi_i,\mu_i & \sigma^2\psi_i & \sigma\psi_i,\varepsilon_i & \sigma\psi_i,x_i \\ \sigma\varepsilon_i,\mu_i & \sigma\varepsilon_i,\psi_i & \sigma^2\varepsilon_i & \sigma\varepsilon_i,x_i \\ \sigma\mu_i,x_i & \sigma\psi_i,x_i & \sigma\varepsilon_i,x_i & \sigma^2x_i \end{pmatrix}$$

In Equation 1.1, μ represents the population intercept, $\bar{\psi}$ the population-level social responsiveness slope to the average social partner' proportion of scrounging x'_t during a given trial t with m social partners, ε the residual social impact exerted by focal individual i on partners j and k , and e the observation-level residual error. Behavioral type and social responsiveness are estimated as among-individual i random intercepts and slopes, respectively. Residual social impact is estimated at the among-individual level and therefore contributes to total phenotypic variance through all social partners (48). We also estimated the among-individual correlation structure among behavioral type, social responsiveness, residual social impact, and the social trait x_i.

$$\phi_i = \frac{\bar{\psi}}{m} * x_i + \varepsilon_i \qquad \textit{Equation 1.2}$$

Individual social impact ϕ_i was subsequently derived from residual social impact ε following Wijnhorst et al. (19). Because social responsiveness is estimated with respect to the average phenotype of an individual's social partners, it was transformed to the equivalent per-partner effect through dividing $\bar{\psi}$ by the number of social partners (m).

$$\sigma^2\phi = \frac{\bar{\psi}}{m}^2 * \sigma^2x_i + \sigma^2\varepsilon_i + 2 * \sigma(x_i,\varepsilon_i) * \frac{\bar{\psi}}{m} \qquad \textit{Equation 1.3}$$

$$\begin{pmatrix} \mu_i \\ \psi_i \\ \phi_i \end{pmatrix} \sim MVN(0, \Omega)\ \Omega: \begin{pmatrix} \sigma^2\mu_i & \sigma\mu_i,\psi_i & \sigma\mu_i,\phi_i \\ \sigma\psi_i,\mu_i & \sigma^2\psi_i & \sigma\psi_i,\phi_i \\ \sigma\phi_i,\mu_i & \sigma\phi_i,\psi_i & \sigma^2\phi_i \end{pmatrix}$$

Posterior social impact variances were calculated from Equation 1.3 using the linearity of (co)variance. This yielded estimates of all (co)variances, and correlations among behavioral type, social responsiveness, and social impact (SI Appendix, Text. S1).

To account for the experimental design, we included random intercepts for trial-identity (n = 1,792) and group-identity (n = 53). Previous analyses showed that additional fixed effects, including trial order and year, had negligible effects on estimates of among-individual variance and covariance (46) and were therefore omitted. Producing and scrounging behavior were analyzed jointly using a bivariate version of Equation 1.1 with multivariate normal random effects, allowing estimation of among-individual, trial-level, and residual covariance structures.

Structural equation models

We used structural equation models (SEMs) to test alternative hypotheses regarding the integration of behavioral type, social responsiveness, and social impact into latent multivariate social strategies (SI Appendix, Fig. S2). In each candidate model, the observed social traits (i) were specified as manifestations of one or more latent variables (η) through factor loadings (Λ) (49). We fitted SEMs using the lavaan package (50) to the posterior standardized best linear unbiased predictors (BLUPs) and their corresponding posterior correlation matrices. This approach provides unbiased estimates of model support and factor loadings while propagating uncertainty from the Bayesian mixed-effects models (SI Appendix, Fig. S3). Each candidate model was fitted to 5,000 random posterior samples, and model support was evaluated using Akaike's Information Criterion (AIC). We summarized the proportion of posterior iterations in which each candidate model provided the best fit, together with the posterior distributions of the estimated factor loadings.

Fitness landscape models

We fitted selection gradient models to quantify how social foraging phenotypes affect relative foraging success. We applied the same selection model to three phenotypic levels: (i) the observed trial-level phenotype (Z); (ii) long-term mean phenotype (behavioral type, μ) estimated using a hierarchical error-in-variables approach (26); and (iii) the posterior median latent multivariate phenotype (η) estimated from the best-fitting structural equation model (Fig. 2A–C). We used individual trial-level relative foraging success ($\omega_{it} = \frac{W_{it}}{\bar{W}}$) as the fitness currency because of its central role in social foraging theory (15, 16). Relative fitness was modeled as a function of the standardized focal phenotypes (natural selection) and social partner phenotypes (social selection) (Equation 2) (5).

$$\omega_{it} = \mu + \mu_i + \beta_1 * Z_i + \frac{1}{2}\gamma_{11} * {Z_i}^2 + \beta_2 * \left(\frac{{Z'}_j + {Z'}_k}{m}\right) + \frac{1}{2}\gamma_{22} * \left(\frac{{Z'}_j + {Z'}_k}{m}\right)^2 + \gamma_{12} * \left(Z_i * \left(\frac{{Z'}_j + {Z'}_k}{m}\right)\right) + T_t + e_{it} \quad \textit{Equation 2}$$

Directional (β) and quadratic (γ) selection gradients quantified natural selection acting on the focal phenotype (β_1, γ_{11}) and social selection acting through the phenotype of social partners (β_2, γ_{22}). The interaction term (γ_{12}) quantified correlational selection between focal and social partner phenotypes,

representing the frequency-dependent fitness consequences of expressing a given phenotype in different social environments (15, 16). We included random intercepts for focal identity $\mu_i$and trial identity T_t to account for repeated observations.

To tease apart how social responsiveness and impact mediate mismatches of behavioral types to the fitness peak, we fitted a joint model with the phenotypic selection gradient and the bivariate producing-scrounging model. We calculated the proportion of scrounging events based on the producing and scrounging BLUPS under two scenarios: 1) μ_i; 2) $\mu_i\ \psi_i\ \varepsilon_{jk}$. Based upon these scenarios, we calculated signed, absolute and Euclidean distance to the peak and their predicted foraging success based on the predicted focal and social partner phenotype.

Data & code availability.

Data and code for analyses are available at:

https://github.com/C-dG/PS_Psi_Phi_W

Acknowledgements & Funding

We thank Jørgen Søraker, Ådne Messel Nafstad, Markus Drangsland, Martin Køber Guldvik, Rok Movh, Sophie Larsson and Tuva Zeiner-Henriksen for their help during the fieldwork.

All experimental procedures conformed with the ethical guidelines concerning the capture and use of animals in research and were approved by the Norwegian Food Safety Authority (FOTS ID 29007) and the Norwegian Bird Ringing Centre.

This work was supported by funding from the German Science Foundation (DI 1694 5–1) for NJD, and the Research Council of Norway (RCN, 325826) for YGA, (RCN, 302619) for HJ, and was also partly supported by the RCN's Centres of Excellence funding scheme (RCN, 223257).

References

1. P. Edelaar, D. I. Bolnick, Appreciating the multiple processes increasing individual or population fitness. *Trends Ecol. Evol.* **34**, 435–446 (2019).

2. P. Edelaar, J. Otsuka, V. J. Luque, A generalised approach to the study and understanding of adaptive evolution. *Biol. Rev.* **98**, 352–375 (2023).

3. M. Nicolaus, P. Edelaar, Comparing the consequences of natural selection, adaptive phenotypic plasticity, and matching habitat choice for phenotype–environment matching, population genetic structure, and reproductive isolation in meta-populations. *Ecol. Evol.* **8**, 3815–3827 (2018).

4. D. A. Baum, *et al.*, *The Princeton Guide to Evolution* (Princeton University Press, 2017).

5. R. Lande, S. J. Arnold, The measurement of selection on correlated characters. *Evol.* **37**, 1210–1226 (1983).

6. E. I. Svensson, Phenotypic selection in natural populations: what have we learned in 40 years? *Evol* **77**, 1493–1504 (2023).

7. D. H. Nussey, E. Postma, P. Gienapp, M. E. Visser, Selection on heritable phenotypic plasticity in a wild bird Population. *Science* **310**, 304–306 (2005).

8. C. K. Ghalambor, J. K. McKAY, S. P. Carroll, D. N. Reznick, Adaptive versus non-adaptive phenotypic plasticity and the potential for contemporary adaptation in new environments. *Funct. Ecol.* **21**, 394–407 (2007).

9. N. W. Bailey, Evolutionary models of extended phenotypes. *Trends Ecol. Evol.* **27**, 561–569 (2012).

10. J. F. Odling-Smee, K. N. Laland, Niche construction. *The American Naturalist* **147**.

11. C. Camacho, A. Sanabria-Fernández, A. Baños-Villalba, P. Edelaar, Experimental evidence that matching habitat choice drives local adaptation in a wild population. *Proc Biol Sci* **287**, 20200721 (2020).

12. Y. G. Araya-Ajoy, D. F. Westneat, J. Wright, Pathways to social evolution and their evolutionary feedbacks. *Evolution* **74**, 1894–1907 (2020).

13. J. M. McNamara, F. J. Weissing, "Evolutionary game theory" in *Social Behaviour: Genes, Ecology and Evolution*, (Cambridge University Press, 2010).

14. A. J. Moore, E. D. III Brodie, J. B. Wolf, Interacting phenotypes and the evolutionary process I: Direct and indirect genetic effects on social interactions. *Evolution* **51**, 1352–1362 (1997).

15. L.-A. Giraldeau, F. Dubois, "Social foraging and the study of exploitative behavior" in *Advances in the Study of Behavior*, (Academic Press, 2008), pp. 59–104.

16. L.-A. Giraldeau, T. Caraco, *Social foraging theory* (Princeton University Press, 2000).

17. N. J. Dingemanse, Y. G. Araya-Ajoy, Interacting personalities: Behavioural ecology meets quantitative genetics. *Trends Ecol. Evol.* **30**, 88–97 (2015).

18. C. de Groot, *et al.*, The importance of distinguishing individual differences in 'social impact' versus 'social responsiveness' when quantifying indirect genetic effects on the evolution of social plasticity. *Neurosci. Biobehav. Rev.* **144**, 104996 (2023).

19. R. E. Wijnhorst, C. de Groot, Y. G. Araya-Ajoy, J. Wright, N. J. Dingemanse, Decomposing social interactions: A statistical method for estimating social impact and social responsiveness. *J. Evol. Biol.* (2026).

20. J. W. McGlothlin, A. J. Moore, J. B. Wolf, E. D. Brodie III, Interacting phenotypes and the evolutionary process III. Social evolution. *Evol.* **64**, 2558–2574 (2010).

21. F. Santostefano, M. Moiron, A. Sánchez-Tójar, D. N. Fisher, Indirect genetic effects increase the heritable variation available to selection and are largest for behaviors: A meta-analysis. *Evolution Letters* (2024). https://doi.org/10.1093/evlett/qrae051.

22. P. Bijma, W. M. Muir, J. A. M. Van Arendonk, Multilevel selection 1: Quantitative genetics of inheritance and response to selection. *Genetics* **175**, 277–288 (2007).

23. A. M. Bell, S. J. Hankison, K. L. Laskowski, The repeatability of behaviour: A meta-analysis. *Animal Behaviour* **77**, 771–783 (2009).

24. L. M. Aplin, J. Morand-Ferron, Stable producer–scrounger dynamics in wild birds: sociability and learning speed covary with scrounging behaviour. *Proceedings of the Royal Society B: Biological Sciences* **284**, 20162872 (2017).

25. M. David, *et al.*, Individual differences in behavioral consistency are related to sequential access to resources and body condition in a producer-scrounger game. *Front. Ecol. Evol.* **2** (2014).

26. J. S. Martin, Y. G. Araya-Ajoy, N. J. Dingemanse, A. J. Wilson, D. Westneat, Estimating (non)linear selection on reaction norms: A general framework for labile traits. *Ecol. Evol.* (2025). https://doi.org/10.1002/ece3.72298.

27. B. Class, *et al.*, Disentangling nonrandom assortment, indirect effects, and joint plasticity as causes of phenotypic (dis)similarity between social partners. *J. Evol. Biol.* **38**, 1082–1092 (2025).

28. P. C. Phillips, S. J. Arnold, Visualizing multivariate selection. *Evolution* **43**, 1209–1222 (1989).

29. J. R. Stinchcombe, A. F. Agrawal, P. A. Hohenlohe, S. J. Arnold, M. W. Blows, Estimating nonlinear selection gradients using quadratic regression coefficients: Double or nothing. *Evol* **62**, 2435–2440 (2008).

30. Y. G. Araya-Ajoy, N. J. Dingemanse, Characterizing behavioural 'characters': An evolutionary framework. *Proceedings of the Royal Society B: Biological Sciences* **281**, 20132645 (2014).

31. N. J. Dingemanse, N. A. Dochtermann, Quantifying individual variation in behaviour: Mixed-effect modelling approaches. *Journal of Animal Ecology* **82**, 39–54 (2013).

32. C. A. Botero, F. J. Weissing, J. Wright, D. R. Rubenstein, Evolutionary tipping points in the capacity to adapt to environmental change. *Proceedings of the National Academy of Sciences* **112**, 184–189 (2015).

33. R. Lande, Adaptation to an extraordinary environment by evolution of phenotypic plasticity and genetic assimilation. *Journal of Evolutionary Biology* **22**, 1435–1446 (2009).

34. L.-M. Chevin, R. Lande, G. M. Mace, Adaptation, plasticity, and extinction in a changing environment: Towards a predictive theory. *PLOS Biology* **8**, e1000357 (2010).

35. F. Santostefano, A. J. Wilson, Y. G. Araya-Ajoy, N. J. Dingemanse, Interacting with the enemy: Indirect effects of personality on conspecific aggression in crickets. *Behav. Ecol.* **27**, 1235–1246 (2016).

36. J. A. Anderson, *et al.*, High social status males experience accelerated epigenetic aging in wild baboons. *eLife* **10**, e66128 (2021).

37. E. A. Tibbetts, J. Pardo-Sanchez, C. Weise, The establishment and maintenance of dominance hierarchies. *Philos Trans R Soc Lond B Biol Sci* **377**, 20200450.

38. S. A. Frank, Natural selection at multiple scales. *Evol* **79**, 1166–1184 (2025).

39. J. W. Jolles, A. J. King, S. S. Killen, The Role of individual heterogeneity in collective animal behaviour. *Trends in Ecology & Evolution* **35**, 278–291 (2020).

40. D. W. Stephens, J. S. Brown, R. C. Ydenberg, *Foraging: Behavior and Ecology* (University of Chicago Press, 2008).

41. A. J. van Noordwijk, G. de Jong, Acquisition and allocation of resources: Their influence on variation in life history tactics. *Am. Nat.* **128**, 137–142 (1986).

42. M. Moiron, K. L. Laskowski, P. T. Niemelä, Individual differences in behaviour explain variation in survival: A meta-analysis. *Ecology Letters* **23** (2020).

43. A. Mouchet, *et al.*, Heterogeneous selection on exploration behavior within and among West European populations of a passerine bird. *Proceedings of the National Academy of Sciences* **118**, e2024994118 (2021).

44. E. D. Brodie III, P. A. Cook, R. A. Costello, V. A. Formica, Phenotypic assortment changes the landscape of selection. *Journal of Heredity* **113**, 91–101 (2022).

45. Å. M. Nafstad, *et al.*, Spatial variation in the evolutionary potential and constraints of basal metabolic rate and body mass in a wild bird. *J. Evol. Biol.* **36**, 650–662 (2023).

46. C. de Groot, *et al.*, Among-trait covariance and cross-year repeatability for direct and indirect individual effects in producer-scrounger behaviour in wild house sparrows. *J. Evol. Biol.* (2026).

47. B. Carpenter, *et al.*, Stan: A probabilistic programming language. *J. Stat. Softw.* **76**, 1–32 (2017).

48. R. Bergsma, E. Kanis, E. F. Knol, P. Bijma, The Contribution of Social Effects to Heritable Variation in Finishing Traits of Domestic Pigs (Sus scrofa). *Genet.* **178**, 1559–1570 (2008).

49. E. C. Merkle, E. Fitzsimmons, J. Uanhoro, B. Goodrich, Efficient bayesian structural equation modeling in Stan. *J. Stat. Softw.* **100**, 1–22 (2021).

50. Y. Rosseel, lavaan: An R Package for Structural Equation Modeling. *J. Stat. Softw.* **048** (2012).

Supporting text S1 Equations variance & covariance calculation social impact

Covariance estimates of social impact were calculated based on the linearity of covariance, see equations below. Note that social responsiveness $\bar{\psi}$ is estimated with respect to the average phenotype of an individual's social partners. Therefore $\bar{\psi}$ was transformed to the equivalent per-partner effect by dividing $\bar{\psi}$ by the number of social partners (m).

Within character covariance estimation when the social partner' phenotypes consist of a different phenotype than the focal phenotype (x_{jt}/x_{kt}):

Variable1	Variable2	Equation covariance	For correlation
μ_i	ϕ_i	$\sigma(\mu_i, \varepsilon_i) + \bar{\psi} * \sigma(x_i, \mu_i)$	$/\sqrt{(\sigma^2 \mu_i * \sigma^2 \phi_i)}$
ψ_i	ϕ_i	$\sigma(\psi_i, \varepsilon_i) + \bar{\psi} * \sigma(x_i, \psi_i)$	$/\sqrt{(\sigma^2 \psi_i * \sigma^2 \phi_i)}$

Cross-trait covariance estimation when both focal phenotypes share the same social environment (x), which consists of a different phenotype than the focal phenotype (x_{jt}/x_{kt}):

Variable1	Variable2	Equation covariance	For correlation
$\mu_i Z1$	$\phi_i Z2$	$\sigma(\mu_i Z1, \varepsilon_i Z2) + \bar{\psi} Z2 * \sigma(x_i, \mu_i Z1)$	$/\sqrt{(\sigma^2 \mu_i Z1 * \sigma^2 \phi_i Z2)}$
$\psi_i Z1$	$\phi_i Z2$	$\sigma(\psi_i Z1, \varepsilon_i Z2) + \bar{\psi} Z2 * \sigma(x_i, \psi_i Z1)$	$/\sqrt{(\sigma^2 \psi_i Z1 * \sigma^2 \phi_i Z2)}$
$\mu_i Z2$	$\phi_i Z1$	$\sigma(\mu_i Z2, \varepsilon_i Z1) + \bar{\psi} Z1 * \sigma(x_i, \mu_i Z2)$	$/\sqrt{(\sigma^2 \mu_i Z2 * \sigma^2 \phi_i Z1)}$
$\psi_i Z2$	$\phi_i Z1$	$\sigma(\psi_i Z2, \varepsilon_i Z1) + \bar{\psi} Z1 * \sigma(x_i, \psi_i Z2)$	$/\sqrt{(\sigma^2 \psi_i Z2 * \sigma^2 \phi_i Z1)}$
$\phi_i Z1$	$\phi_i Z2$	$\sigma(\varepsilon_i Z1, \varepsilon_i Z2) + \bar{\psi} Z1 * \sigma(x_i, \varepsilon_i Z2) + \bar{\psi} Z2 * \sigma(x_i, \varepsilon_i Z1) + \bar{\psi} Z1 * \bar{\psi} Z2 * \sigma^2 x_i$	$/\sqrt{(\sigma^2 \phi_i Z1 * \sigma^2 \phi_i Z2)}$

Figure S1 Bivariate model correlation matrices

A)

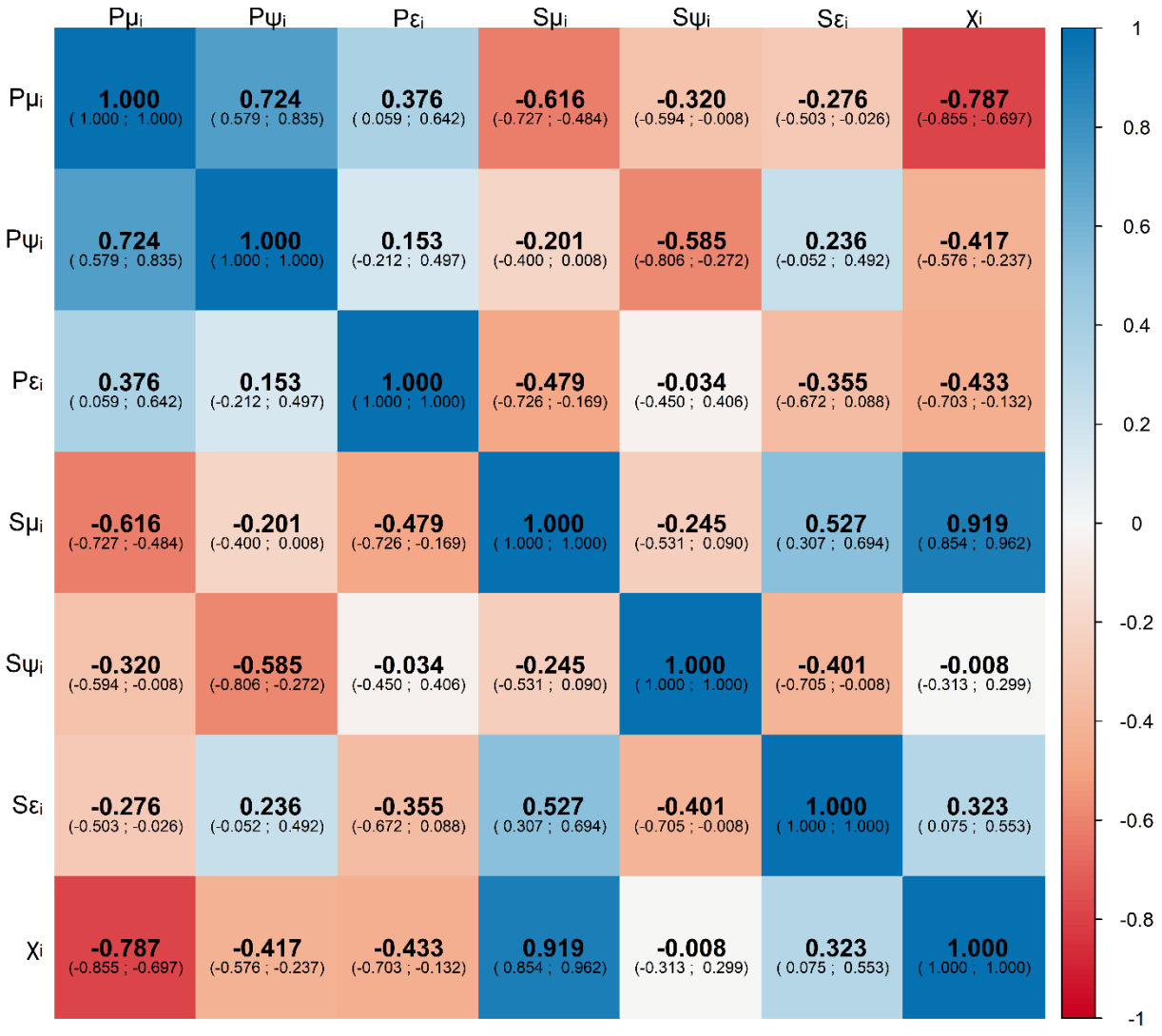

B)

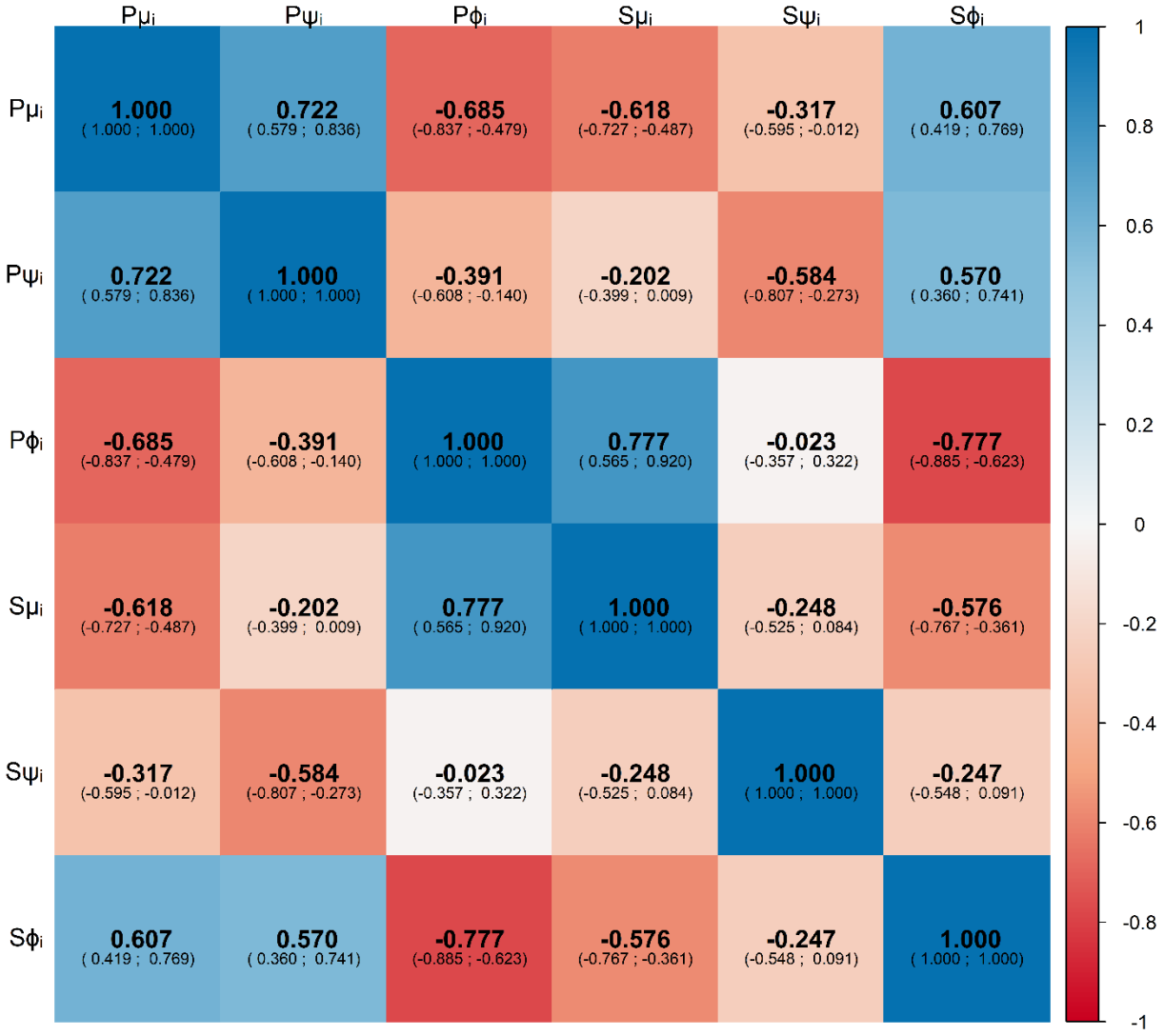

Figure S1 *Correlation matrices estimated at the individual level (i) with median estimates and 95% credible intervals for producing and scrounging behaviors in response to observed partner phenotypes from the bivariate model. The among trial correlation is -0.870 (-0.914 ; -0.823), and the residual correlation is -0.054 (-0.092 ; -0.016). Mu (μ) denotes behavioral type, psi (ψ) denotes social responsiveness, epsilon (ε) denotes residual social impact, x denotes average proportion of scrounging events, and phi (ϕ) denotes social impact. P denotes producing behavior, and S scrounging behavior.* ***A)*** *Correlation matrix estimated by the model.* ***B)*** *derived matrix with social impact correlations (see supporting text S1).*

Figure S2 Structural equation models (SEM) and best fits

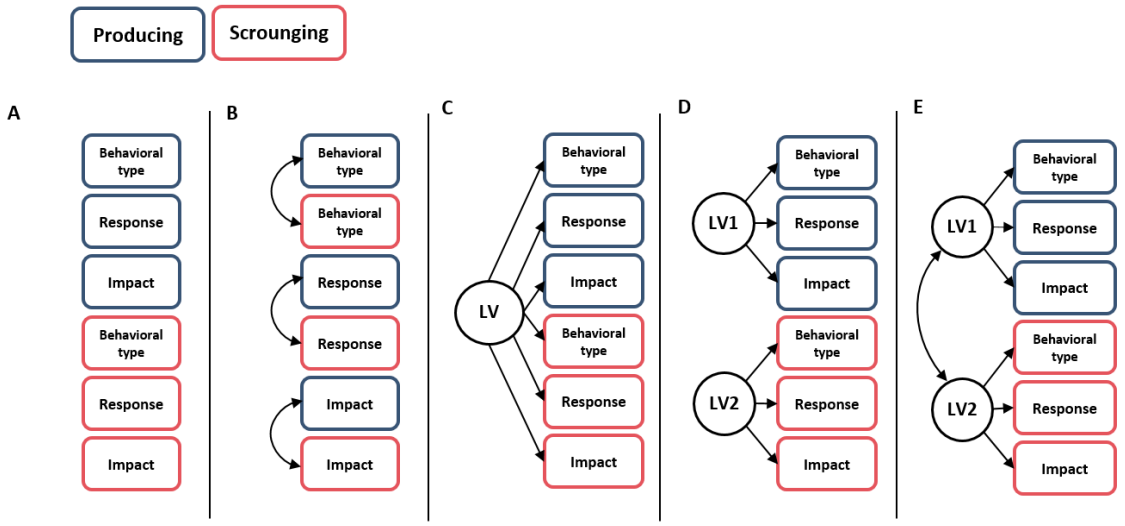

	A	B	C	D	E
BLUP	0	0.02	0.89	0	0.09
Correlation	0	0.02	0.84	0	0.14

Figure S2*. Alternative hypotheses for phenotypic integration structure, corresponding to fitted structural equation models (SEM). Model* ***A*** *posits no integrated phenotypic structure (i.e. all correlations set to zero). Model* ***B*** *posits correlation structure among producer and scrounger behavioral components, but not across behavioral components. Model* ***C*** *posits that producer-scrounger behavioral components are integrated into one underlying latent variable. Model* ***D*** *posits that producer-scrounger behavioral components are integrated into two uncorrelated underlying latent variables. Model* ***E*** *posits that producer-scrounger behavioral components are integrated into two correlated underlying latent variables. The posterior probabilities of each candidate model having the lowest ΔAIC across 5000 producer-scrounger structural equation models are printed below, for models fitted using either individual BLUPS or the correlation matrix. We performed our analyses with these two approaches as both are used in our field of research, here we show that they return the same results. In the text we therefore present results based on just the former. All models converged well, and were positive definite, except model E, which converged well for 4978 and 4975 samples, and had positive definite latent variable matrices for 4320 and 4352 samples for BLUPS and correlations respectively. ΔAIC is based on samples excluding non-converged and non-positive definite samples.*

Figure S3 Structural Equation Modelling (SEM) approach simulations

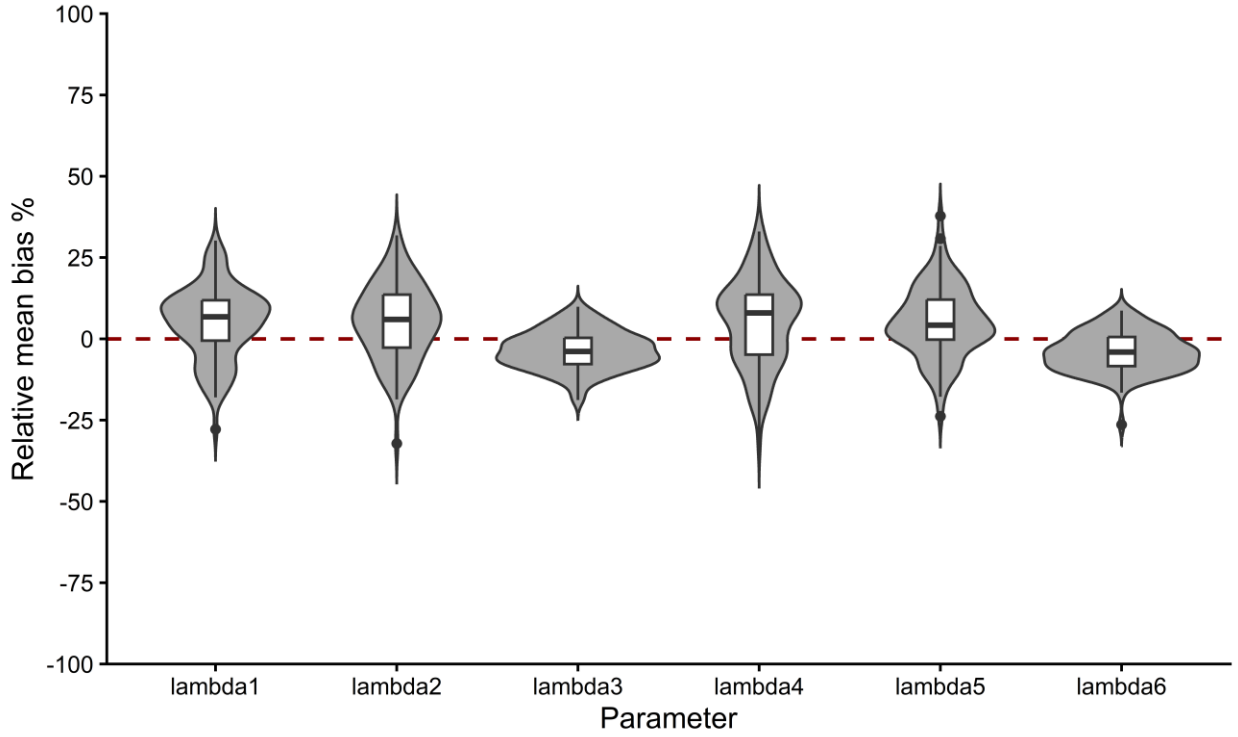

Figure S3*. Relative mean bias of simulated structural equation models based on the BLUP approach described in the methods. The boxplot showing the median estimate, and the violin plots are based on 100 simulated datasets with the structure of the empiric data. Loadings are set to 0.5 for lambda 1-2, and 4-5 (behavioral type and social responsiveness), and 0.75 for lambda 3 and 6 (social impact), reflecting observed effect sizes. The simulations further show that all loadings are estimated with a power of 1, and that the correct model is supported across all 100 datasets with a mean proportion of lowest ΔAIC of 0.98.*

Table S1 Bivariate model estimates table

Table S1 *Bivariate median estimates with 95% credible intervals for producing and scrounging behaviors in response to observed partner phenotypes. Mu (μ) denotes behavioral type, psi (ψ) denotes social responsiveness, epsilon (ε) denotes residual social impact, and phi (ϕ) denotes social impact. Social responsiveness variance and repeatability are conditional on the variance of the covariate (1).*

Variable	Producing	Scrounging
Fixed effects	**β (95% CI)**	**β (95% CI)**
Intercept	1.536 (1.438 ; 1.635)	0.650 (0.585 ; 0.715)
$\bar{\psi}$	2.564 (2.356 ; 2.769)	-2.034 (-2.138 ; -1.925)
Random effects	**σ^2 (95% CI)**	**σ^2 (95% CI)**
μ_i	0.218 (0.172 ; 0.275)	0.063 (0.048 ; 0.082)
ψ_i	0.052 (0.036 ; 0.072)	0.004 (0.001 ; 0.007)
ε_i	0.010 (0.002 ; 0.023)	0.013 (0.007 ; 0.021)
φ_i	0.041 (0.027 ; 0.058)	0.031 (0.021 ; 0.044)
Trial	0.373 (0.307 ; 0.442)	0.462 (0.416 ; 0.511)
Group	0.036 (0.014 ; 0.073)	0.001 (0.000 ; 0.011)
Residual	0.824 (0.782 ; 0.870)	0.257 (0.243 ; 0.271)
P	1.529 (1.447 ; 1.620)	0.815 (0.769 ; 0.865)
Repeatability	**R (95% CI)**	**R (95% CI)**
μ_i	0.143 (0.115 ; 0.175)	0.077 (0.059 ; 0.099)
ψ_i	0.034 (0.024 ; 0.046)	0.004 (0.001 ; 0.009)
ε_i	0.007 (0.001 ; 0.015)	0.016 (0.009 ; 0.026)
φ_i	0.027 (0.018 ; 0.038)	0.038 (0.026 ; 0.054)
Trial	0.244 (0.205 ; 0.282)	0.567 (0.531 ; 0.602)
Group	0.024 (0.009 ; 0.047)	0.001 (0.000 ; 0.014)
Residual	0.539 (0.501 ; 0.579)	0.315 (0.290 ; 0.342)

Table S2 Selection gradient estimates

Table S2 *Median estimates with 95% credible intervals for selection gradient parameters for observed phenotype, behavioral type, and multivariate type based on the median latent variable factor-scores for producer-scrounger behaviors. "1" denotes selection on focal traits and "2" denotes selection by partner traits. Latent variable scores are inverted, so scrounger strategies are positive values compared to Figure 3. Absolute curvature is the Frobenius norm presented in the main text, net curvature is based on the sum of eigenvalues, and provides similar results. Z1* and Z2* represent the optimal focal and social partner phenotypes at the fitness peak.*

Parameter	*Phenotype*	*Behavioral type*	*Multivariate type*
Fixed effects	**β (95% CI)**	**β (95% CI)**	**β (95% CI)**
Intercept	1.139 (1.099 ; 1.178)	1.043 (0.992 ; 1.095)	0.984 (0.943 ; 1.026)
β_1	0.035 (0.014 ; 0.056)	-0.012 (-0.051 ; 0.028)	-0.032 (-0.062 ; -0.001)
β_2	0.049 (0.033 ; 0.066)	-0.028 (-0.050 ; -0.005)	-0.034 (-0.051 ; -0.017)
γ_{11}	-0.177 (-0.214 ; -0.138)	-0.133 (-0.291 ; 0.030)	0.039 (-0.004 ; 0.081)
γ_{22}	-0.115 (-0.142 ; -0.087)	-0.082 (-0.186 ; 0.022)	0.001 (-0.021 ; 0.023)
γ_{12}	-0.070 (-0.090 ; -0.051)	-0.012 (-0.034 ; 0.010)	-0.010 (-0.026 ; 0.007)
Random effects	**σ^2 (95% CI)**	**σ^2 (95% CI)**	**σ^2 (95% CI)**
Individual	0.049 (0.039 ; 0.061)	0.048 (0.038 ; 0.060)	0.048 (0.038 ; 0.060)
Trial	0.068 (0.059 ; 0.077)	0.075 (0.066 ; 0.085)	0.075 (0.066 ; 0.085)
Residual	0.145 (0.138 ; 0.152)	0.146 (0.139 ; 0.154)	0.147 (0.139 ; 0.155)
Landscape parameters	**x (95% CI)**	**x (95% CI)**	**x (95% CI)**
Absolute curvature	*0.234 (0.194 ; 0.274)*	*0.167 (0.044 ; 0.317)*	*0.044 (0.014 ; 0.084)*
Net curvature	*-0.291 (-0.341 ; -0.242)*	*-0.214 (-0.415 ; -0.011)*	*0.040 (-0.009 ; 0.089)*
*Z1**	*0.347 (0.324 ; 0.366)*	*0.319 (0.181 ; 0.424)*	*0.270 (-5.792 ; 5.969)*
*Z2**	*0.377 (0.358 ; 0.402)*	*0.307 (0.122 ; 0.459)*	*-0.479 (-25.547 ; 26.347)*

Table S3 Predicted phenotypes and fitness landscape estimates

Table S3 *Median estimates with 95% credible intervals for predicted distance from the peak, and foraging success. Scenario 1 is based on predicted individual behavioral type values (μ_i), scenario 2 on behavioral type, social responsiveness and residual social impact ($\mu_i + \psi_i xjk + \varepsilon_{jk}$). Estimates are reported on a percentage scale rather than a proportion (i.e. *100). Zi denotes the focal individual phenotype, and Zjk the social environment. Δ denotes the signed distance and Abs Δ the absolute distance from the predicted fitness optimum.* ***A)*** *Estimates per scenario.* ***B)*** *Comparisons between scenarios presented in A. Estimates are based on the second to the first scenario denoted in the columns. Individual variation, cross-context, and intercept-slope correlations are estimated with linear mixed models in lme4 per posterior sample.*

A)

	1: Behavioral type	2: Multivariate phenotype
Means	**$\bar{x}$ (95% CI)**	**$\bar{x}$ (95% CI)**
Δ Zi	3.824 (1.712 ; 6.508)	5.113 (3.071 ; 7.721)
Δ Zjk	0.827 (-1.877 ; 3.305)	2.030 (-0.600 ; 4.353)
Abs Δ Zi	6.781 (6.038 ; 8.061)	14.255 (13.621 ; 15.043)
Abs Δ Zjk	4.183 (3.755 ; 4.939)	8.982 (8.536 ; 9.533)
Euclidean distance	8.642 (7.747 ; 9.914)	17.909 (17.145 ; 18.793)
Foraging success	112.960 (108.877 ; 116.900)	110.812 (106.809 ; 114.733)
Individual variance	**σ^2_I (95% CI)**	**σ^2_I (95% CI)**
Δ Zi	62.575 (52.502 ; 73.691)	89.143 (78.680 ; 100.310)
Δ Zjk	12.213 (9.439 ; 15.494)	2.842 (0.783 ; 5.954)
Abs Δ Zi	31.821 (23.350 ; 43.819)	15.490 (10.390 ; 23.545)
Abs Δ Zjk	2.643 (1.607 ; 5.653)	0.127 (0.000 ; 0.607)
Euclidean distance	29.952 (20.844 ; 42.169)	12.915 (8.352 ; 20.123)
Foraging success	3.751 (1.739 ; 7.467)	1.986 (1.170 ; 3.061)

B)

	ΔScenario1-2
Means	**$\bar{x}$ (95% CI)**
Δ Zi	1.285 (0.633 ; 1.921)
Δ Zjk	1.197 (0.548 ; 1.831)
Abs Δ Zi	7.433 (6.660 ; 8.120)
Abs Δ Zjk	4.783 (4.187 ; 5.308)
Euclidean distance	9.246 (8.298 ; 10.143)
Foraging success	-2.147 (-3.017 ; -1.287)
Individual variance	**σ^2_I (95% CI)**
Δ Zi	26.547 (21.875 ; 31.324)
Δ Zjk	-9.285 (-12.084 ; -6.436)
Abs Δ Zi	-16.239 (-22.199 ; -11.382)
Abs Δ Zjk	-2.508 (-5.359 ; -1.415)
Euclidean distance	-16.868 (-24.722 ; -10.384)
Foraging success	-1.746 (-4.589 ; -0.390)
Cross-context correlation	**r (95% CI)**
Δ Zi	0.949 (0.928 ; 0.965)
Δ Zjk	0.787 (0.487 ; 0.956)
Abs Δ Zi	0.828 (0.740 ; 0.887)
Abs Δ Zjk	0.264 (-0.110 ; 0.611)
Euclidean distance	0.816 (0.706 ; 0.889)
Foraging success	0.731 (0.528 ; 0.830)
Intercept-slope correlation	**r (95% CI)**
Δ Zi	0.426 (0.314 ; 0.542)
Δ Zjk	-0.620 (-0.814 ; -0.348)
Abs Δ Zi	-0.660 (-0.732 ; -0.567)
Abs Δ Zjk	-0.686 (-0.841 ; -0.463)
Euclidean distance	-0.665 (-0.762 ; -0.528)
Foraging success	-0.640 (-0.799 ; -0.455)

Supporting references

1. H. Schielzeth, S. Nakagawa, Conditional repeatability and the variance explained by reaction norm variation in random slope models. *Methods in Ecology and Evolution* **13**, 1214–1223 (2022).